Antibody−Metalloporphyrin Catalytic Assembly Mimics Natural Oxidation Enzymes

Shai Nimri‡ and Ehud Keinan*,‡,†

Contribution from the Department of Chemistry and Institute of Catalysis Science and Technology, Technion-Israel Institute of Technology, Technion City, Haifa 32000, Israel, and Department of Molecular Biology and The Skaggs Institute for Chemical Biology, The Scripps Research Institute, 10550 North Torrey Pines Road, La Jolla, California 92037

Received February 1, 1999

Abstract: An antibody−metalloporphyrin assembly that catalyzes the enantioselective oxidation of aromatic sulfides to sulfoxides is presented. Antibody SN37.4 was elicited against a water-soluble tin(IV) porphyrin containing an axial α-naphthoxy ligand. The catalytic assembly comprising antibody SN37.4 and a ruthenium(II) porphyrin cofactor exhibited typical enzyme characteristics, such as predetermined oxidant and substrate selectivity, enantioselective delivery of oxygen to the substrate, and Michaelis−Menten saturation kinetics. This assembly, which promotes a complex, multistep catalytic event, represents a close model of natural heme-dependent oxidation enzymes.

Introduction

Understanding the chemistry of biological oxidation reactions is key to the understanding of many natural processes, including biosynthesis of endogenous compounds and biodegradation of xenobiotics.[1] Most of these reactions are catalyzed by highly evolved assemblies of proteins and cofactors, such as the family of cytochrome P-450 and other metalloporphyrin-containing enzymes.[2] The mechanistic details of such enzymatic systems have been the subject of extensive research efforts, led by the need to verify postulated theories and resolve controversial issues.[2−4] These studies have included intact biological systems[2] and mutated enzymes,[3] as well as non-protein chemical analogues of the metalloporphyrin cofactor.[4]

The science of catalytic antibodies[5] has created novel opportunities from which we can learn about these complicated enzymatic systems. It has been previously shown that antibodies which were elicited against a specific metalloporphyrin hapten exhibit higher affinity to the original hapten than to the same porphyrin bound to other metals.[6] *N*-Methylmesoporphyrin IX has been used as a hapten to produce antibodies that mimic the ferrocatalase activity.[7] The same antibodies have presented peroxidase activity when iron(III)−mesoporphyrin IX was utilized as a cofactor.[8] Similar catalysis, with unpredicted substrate selectivity, has been reported for another antibody−metalloporphyrin complex.[9] We have already shown that appropriately designed antibodies with metalloporphyrin cofactors can mimic the catalytic activity of the P-450 enzymes.[10]

A particularly intriguing challenge is how to use the catalytic antibody technology to create a more complicated protein active site, with a higher degree of similarity to the enzymatic systems. Such an active site should accommodate not only the metalloporphyrin cofactor but also the oxygen donor and the organic substrate in the correct orientation for reaction. Here we report on the first achievement of this task. A tin porphyrin hapten bearing an α-naphthoxy axial ligand was used as a structural analogue of the transition state that includes all components of the catalytic event. The resultant monoclonal antibody specifically binds a ruthenium porphyrin cofactor to form a novel catalytic assembly that exhibits predesigned activity in sulfide oxygenation reactions. This assembly features typical enzyme characteristics, including oxidant and substrate selectivity, enantioselective delivery of oxygen to the substrate, and Michaelis−Menten saturation kinetics.

* To whom correspondence should be addressed. Phone: (619) 784-8511. Fax: (619) 784-8732. E-mail: Keinan@Scripps.edu.

‡ Technion-Israel Institute of Technology.

† The Scripps Research Institute.

(1) (a) Walsh, C.; Latham, J. *J. Protein Chem.* **1986**, *5*, 79. (b) Holland, H. L. *Chem. Rev.* **1988**, *88*, 473. (c) Jakoby, W. B.; Ziegler, D. M. *J. Biol. Chem.* **1990**, *265*, 20715.

(2) (a) *The Porphyrins*; Dolphin, D., Ed.; Academic Press: New York, 1978; Vol. VII, Chapter 6. (b) *Cytochrome P-450: Structure, Mechanism and Biochemistry*; Ortiz de Montellano, P. R., Ed.; Plenum Press: New York, 1986. (c) Watanabe, Y.; Oae, S.; Iyanagi, T. *Bull. Chem. Soc. Jpn.* **1982**, *55*, 188.

(3) (a) Ozaki, S.; Ortiz de Montellano, P. R. *J. Am. Chem. Soc.* **1995**, *117*, 7056. (b) Ozaki, S.; Matsui, T.; Watanabe, Y. *J. Am. Chem. Soc.* **1996**, *118*, 9784.

(4) A few examples: (a) McMurry, T. J.; Groves, J. T. In ref 2b; Chapter 1. (b) Collman, J. P.; Brauman, J. I.; Hampton, P. D.; Hiroo, T.; Bohle, D. S.; Hembre, R. T. *J. Am. Chem. Soc.* **1990**, *112*, 7980. (c) Ostovic, D.; Bruice, T. C. *Acc. Chem. Res.* **1992**, *25*, 314. (d) Meunier, B. *Chem. Rev.* **1992**, *92*, 1411. (e) Collman. J. P.; Zhang, X.; Lee, V. J.; Uffelman, E. S.; Brauman, J. I. *Science* **1993**, *261*, 1404. (f) Gross, Z.; Nimri, S. *J. Am. Chem. Soc.* **1995**, *117*, 8021. (g) Gross, Z.; Ini, S. *J. Org. Chem.* **1997**, *62*, 5514.

(5) (a) Schultz, P. G.; Lerner, R. A. *Science* **1995**, *269*, 1835. (b) Jacobsen, J. R.; Schultz, P. G. *Curr. Opin. Struct. Biol.* **1995**, *5*, 818. (c) MacBeath, G.; Hilvert, D. *Chem., Biol.* **1996**, *3*, 433. (d) Keinan, E.; Lerner, R. A. *Isr. J. Chem.* **1996**, *36*, 113. (e) Thomas, N. R. *Nat. Prod. Rep.* **1996**, 479.

(6) Schwabacher, A. W.; Weinhouse, M. I.; Auditor M.-T. M.; Lerner, R. A. *J. Am. Chem. Soc.* **1989**, *111*, 2344.

(7) Cochran, A. G.; Schultz, P. G. *Science* **1990**, *249*, 781.

(8) Cochran, A. G.; Schultz, P. G. *J. Am. Chem. Soc.* **1990**, *112*, 9414.

(9) Harada, A.; Fukushima, H.; Shiotzuki, K.; Yamaguchi, H.; Oka, F.; Kamachi, M. *Inorg. Chem.* **1997**, *36*, 6099.

(10) (a) Keinan, E.; Sinha, S. C.; Sinha-Bagchi, A.; Benory, E.; Ghozi, M. C.; Eshhar, Z.; Green, B. S. *Pure Appl. Chem.* **1990**, *62*, 2013. (b) Keinan, E.; Benory, E.; Sinha, S. C.; Sinha-Bagchi, A.; Eren, D.; Eshhar, Z.; Green, B. S. *Inorg. Chem.* **1992**, *31*, 5433.

10.1021/ja990314q CCC: $18.00
Published on Web 09/18/1999

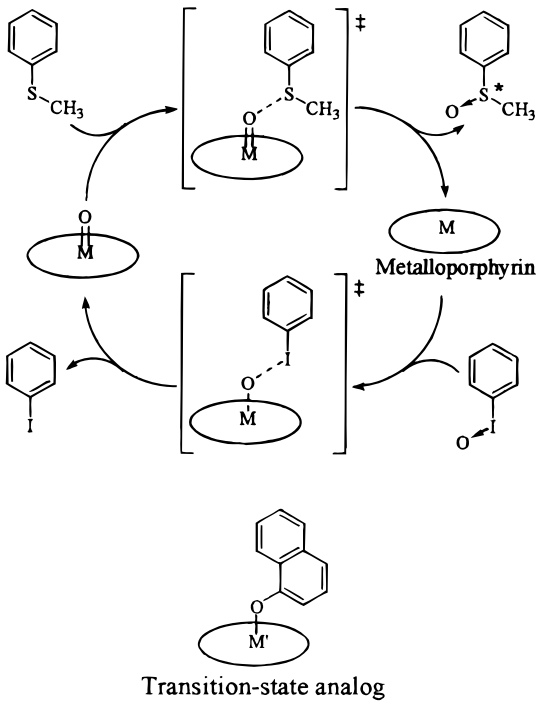

Figure 1. Catalytic cycle of metalloporphyrin-catalyzed sulfoxidation of thioanisole and the proposed transition state analogue.

Results and Discussion

The wide variety of metalloporphyrin-catalyzed oxygenation reactions, including epoxidation, hydroxylation, and sulfoxidation, share a similar transition-state structure. It is commonly accepted that, in these transition states, the organic substrate is positioned in close proximity to the oxygen atom of a high-valent metallo-oxo-porphyrin component,[11,12] as illustrated in the sulfoxidation of thioanisole (Figure 1). Accordingly, a key element in the design of our transition-state analogue was the positioning of an α-naphthoxy ligand at an axial coordination site of a metalloporphyrin core. This ligand could mimic the size and relative orientation of the thioanisole substrate in the transition state, as well as the shape and location of iodosylbenzene (PhIO), a frequently used reagent for the oxidation of the metalloporphyrin (Figure 1).[12a]

The design and synthesis of the required hapten is a nontrivial task, because in addition to the demanded analogy to the transition state, this hapten should also have a considerable hydrolytic stability under the physiological conditions during the immunization process. Our choice of a tin porphyrin hapten, tcpp-Sn-(α-naphthoxy)Cl (**P1**, Chart 1) [tcpp = *meso*-tetrakis-(4-carboxyphenyl)porphyrin], is based on using a main-group metal in order to increase the covalent character of the metal−oxygen bond and thereby enhance its hydrolytic stability. The hydrophobic nature of the axial α-naphthoxy ligand further increases the hapten's kinetic stability under aqueous conditions.[13] The carboxylic substituents on the porphyrin periphery were designed to render this highly hydrophobic hapten water soluble and also to allow for conjugation with the carrier protein.

(11) For high-valent metallo-oxo-porphyrins, see: (a) Groves, J. T.; Haushalter, R. C.; Nakamura, M.; Nemo, T. E.; Evans, B. J. *J. Am. Chem. Soc.* **1981**, *103*, 2884. (b) Groves, J. T.; Quinn, R. *Inorg. Chem.* **1984**, *23*, 3846−3853. (c) Groves, J. T.; Stern, M. K. *J. Am. Chem. Soc.* **1987**, *109*, 3812.

(12) For postulated transition states, see: (a) Groves, J. T.; Nemo, T. E. *J. Am. Chem. Soc.* **1983**, *105*, 5786. (b) Groves, J. T.; Nemo, T. E. *J. Am. Chem. Soc.* **1983**, *105*, 6243. (c) Groves, J. T.; Han, Y.; Engen, D. V. *J. Chem. Soc., Chem. Commun.* **1990**, 436−437. (d) Reference 2c.

(13) Buchler, J. W. In *The Porphyrins*; Dolphin, D., Ed.; Academic Press: New York, 1978; Vol. I, Chapter 10.

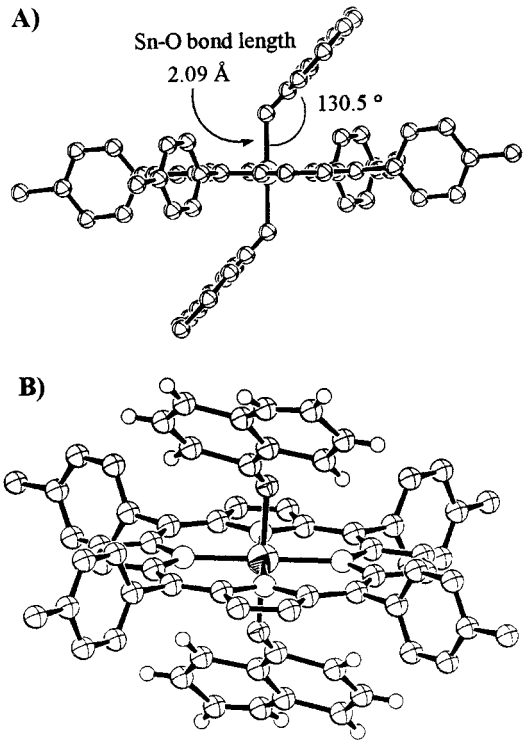

Figure 2. X-ray structure of [*meso*-tetrakis(4-tolyl)porphinato]tin(IV) di(α-naphthoxide) (**P3**): (A) side view and (B) top view, including the α-naphthoxy hydrogen atoms (calculated).

Chart 1. Metalloporphyrins

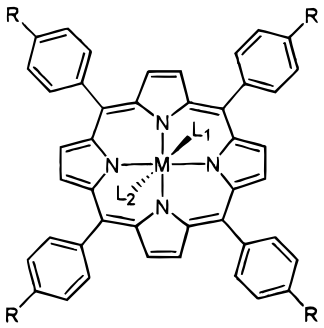

P1) M = Sn(IV), R = CO_2H, L_1 = α-naphthoxy, L_2 = Cl

P2) M = Sn(IV), R = CO_2H, $L_1 = L_2$ = Cl

P3) M = Sn(IV), R = CH_3, $L_1 = L_2$ = α-naphthoxy

P4) M = Sn(IV), R = Br, $L_1 = L_2$ = α-naphthoxy

P5) M = Ru(II), R = CO_2H, L_1 = CO, no L_2

Hapten **P1** was synthesized by reacting tcpp-Sn-Cl_2 (**P2**, Chart 1) with excess α-naphthol in boiling pyridine. Compound **P1** was characterized by ^{1}H NMR spectroscopy, in comparison with the organic-soluble analogues, **P3** and **P4** (Chart 1), and by solving the molecular structure of **P3** using X-ray crystallography (Figure 2). Hapten **P1** was found to be satisfactorily stable (by ^{1}H NMR, see Supporting Information) during 48 h under physiological conditions (50 mM phosphate buffer, pH 7.4, 100 mM NaCl, 37 °C).

The hapten was conjugated with carrier proteins, keyhole limpet hemocyanin (KLH) and bovine serum albumin (BSA), using common procedures.[14] Balb/C mice were immunized with

(14) Staros, J. V.; Wright, R. W.; Swingle, D. M. *Anal. Biochem.* **1986**, *156*, 220.

Chart 2. Substrates

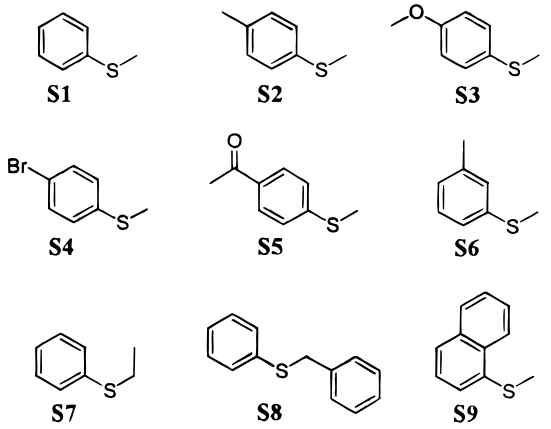

the KLH conjugate, and monoclonal antibodies were produced using accepted protocols.[15] Three antibodies, which exhibited the highest affinities toward the BSA conjugate ($K_d < 10^{-7}$ M) by competition ELISA tests,[16] were produced from ascites fluid in sufficient amounts for the kinetic studies. Antibody SN37.4 was selected for more detailed study on the basis of the highest enantioselectivity in sulfoxidation reactions (vide infra). Interestingly, the affinity of antibody SN37.4 to hapten **P1** ($K_d = 5 \times 10^{-8}$ M, estimated by competition ELISA) was found to be 2 orders of magnitude higher than its affinity to the dichlorotin porphyrin **P2** ($K_d = 5 \times 10^{-6}$ M). These results indicate that the antibody recognizes not only the porphyrin ring but also the axial α-naphthoxy ligand.

The oxidation reaction of sulfides **S1**−**S7** (Chart 2) to the corresponding chiral sulfoxides was carried out with PhIO in the presence of antibody SN37.4 and the Ru(II) porphyrin tcpp-Ru-CO (**P5**, Chart 1). The reaction parameters (e.g., pH 9.0) were chosen primarily on the basis of maximal enantioselectivity.[17] Excess antibody with respect to the metalloporphyrin (13.4:1 molar ratio) was used in order to maximize the fraction of metalloporphyrin molecules that resides within the antibody's binding site at equilibrium. Under these conditions, we studied the sulfoxidation reaction kinetics with increasing substrate concentrations. Saturation kinetics with excellent fit to the Michaelis−Menten model was observed, as demonstrated for thioanisole (**S1**) (Figure 3). The kinetic parameters k_{cat} and K_M and the products' ee values are given in Table 1.

In control experiments, we added the inert tin porphyrin **P2** (7.5-fold molar excess with respect to the antibody) to the reaction mixtures. First-order kinetic behavior rather than saturation kinetics was observed, and the sulfoxide products were obtained in the form of a racemic mixture. Similar results were recorded when an irrelevant protein, such as BSA, was used instead of antibody SN37.4 (see k_{BSA} in Table 1). In another control experiment, we examined the oxidation of these sulfides

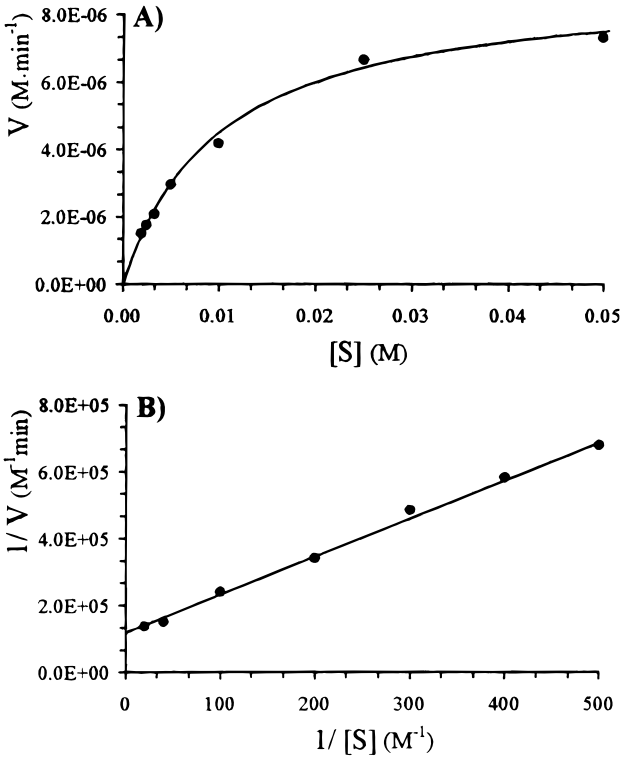

Figure 3. (A) Initial velocity of the sulfoxidation reaction of **S1** catalyzed by the assembly comprising antibody SN37.4 and tcpp-Ru-CO (**P5**), as a function of the substrate's concentration. (B) Lineweaver−Burk plot of this reaction.

Table 1. Kinetic Parameters and ee Values for Sulfoxidation Reactions of Substrates **S1**−**S7**, Catalyzed by the Assembly of Antibody SN37.4 with the Ruthenium Porphyrin **P5**, and First-Order Rate Constants of the Control Experiments

	k_{cat} (min^{-1})[a]	K_M ($\times 10^{-2}$ M)[a]	ee (%)[a,b]	K_{BSA} ($\times 10^{-4}$ min^{-1})[c]	k_{uncat} ($\times 10^{-5}$ min^{-1})[d]
S1	24.0	1.0	43	8.4	8.7
S2	34.7	1.9	32	13	16
S3	174.3	2.0	27	59	27
S4	17.1	1.9	27	4.4	2.8
S5	8.8	2.3	24	2.2	1.8
S6	33.0	2.6	20	9.1	10
S7	25.3	2.4	21	10	10

[a] Corrected for the background reactions (vide infra). [b] In all cases, the (*S*)-sulfoxide was the more abundant enantiomer. [c] k_{BSA} is defined as the rate constant of a reaction where BSA was used instead of antibody SN37.4. [d] k_{uncat} is defined as the rate constant of a reaction carried out in the presence of either SN37.4 or BSA but in the absence of the metalloporphyrin.

by PhIO with SN37.4 in the absence of any metalloporphyrin. Again, a first-order kinetic behavior was observed (see k_{uncat} in Table 1), and only racemic sulfoxides were produced. These results confirm that the catalytic assembly, comprising SN37.4 and specifically bound **P5**, is responsible for both phenomena of saturation kinetics and enantioselectivity.

In contrast to the cases of substrates **S1**−**S7**, neither enantioselectivity nor saturation kinetics could be detected in the sulfoxidation reactions of the sterically larger sulfides **S8** and **S9** (Chart 2). This substrate discrimination may be understood on the basis of the molecular shape and size of the sulfides relative to that of the α-naphthyl group in the hapten. While substrates **S1**−**S7** can fit into a binding pocket defined by the α-naphthyl moiety, sulfides **S8** and **S9** are too large to enter that site. Consequently, their oxidation is catalyzed not by the antibody−metalloporphyrin assembly but by the free **P5** mol-

(15) Goding, J. W. *Monoclonal Antibodies: Principles and Practice*, 2nd ed.; Academic Press: New York, 1986.

(16) Clark, B.; Eengvali, E. In *ELISA: Theoretical and Practical Aspects in Enzyme-Immunuassay*; Mggio, E. T., Ed.; CRC Press: Boca Raton, FL, 1980; Chapter 8.

(17) For example, we examined two other metalloporphyrins, tcpp-Fe-Cl and tcpp-Mn-Cl, that yielded lower ee values (maximum of 10% and 4%, respectively, in the sulfoxidation of thioanisole, **S1**).

(18) (a) Correction of the observed reaction velocities was carried out using the following equation: $V_{assembly} = V_{observed} - [k_{uncat} + 0.25(k_{BSA} - k_{uncat})][S]$, where $V_{assembly}$ is the velocity of the reaction that was catalyzed within the assembly's active site. (b) Correction of the observed ee values was carried out using the following equation: $ee_{assembly} = ee_{observed}/(V_{assembly}/V_{observed})$. (c) The catalytic assembly's concentration was considered as 75% of the metalloporphyrin used.

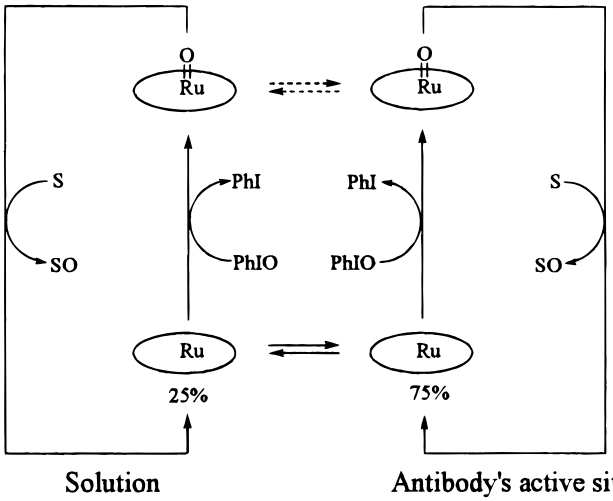

Figure 4. Schematic description of the catalytic system.

ecules that coexist in equilibrium with the antibody-bound **P5**. Our hypothesis was further supported by kinetic measurements. The porphyrin-catalyzed sulfoxidation rates of **S8** and **S9** in the presence of antibody SN37.4 were found to be equal to the rates of control reactions in which we used BSA instead of the antibody and only 25% of the metalloporphyrin. Thus, we conclude that the equilibrium distribution of **P5** between the antibody binding site and the solution is 75:25, respectively. We used this ratio to correct our observed data for the background reactions prior to determination of the kinetic parameters and ee values (Table 1).[18]

Evidently, the observed enantioselectivity indicates that the sulfoxidation step occurs within the protein active site. Yet, considering the general catalytic cycle (Figure 4), it is not clear whether the other steps, particularly the metalloporphyrin oxygenation reaction, also take place within the active site. In principle, this oxygen transfer from the oxidant to the ruthenium atom could occur in solution, followed by binding of the resultant oxoruthenium intermediate to the antibody. To examine this issue, we repeated the above-described oxidation of **S1** using the same procedures, except $NaIO_4$ was employed as an oxidant instead of PhIO. Since it seems unlikely that the antibody would specifically bind a tetrahedral, negatively charged species such as the periodate ion, the reaction between **P5** and $NaIO_4$ in the presence of SN37.4 is expected to occur only in solution. Nevertheless, if the binding of the resultant oxoruthenium intermediate to the antibody is faster than the sulfide oxygenation step, then enantioselective sulfoxidation should still be observed. Conversely, if binding of the oxoruthenium intermediate to the antibody is slower than the sulfide oxygenation, then a racemic sulfoxide will be produced. In fact, treatment of **S1** with $NaIO_4$ in the presence of **P5** and antibody SN37.4 produced the corresponding racemic sulfoxide. Furthermore, kinetic studies with $NaIO_4$ confirmed that only unbound porphyrin molecules catalyzed this reaction. Thus, it is safe to conclude that, when an appropriate oxidant such as PhIO is used, the entire catalytic cycle, including both oxygen-transfer steps, takes place within the active site. Consequently, the antibody−metalloporphyrin assembly should be considered as an inseparable catalytic device.

The promiscuity of the catalytic assembly with respect to small substituents on the thioanisole ring (Table 1) allowed for a linear free energy relationship study of the sulfoxidation reaction. A Hammett plot with the k_{cat} values of **S1** and its derivatives **S2**−**S6** shows a good linear correlation ($\rho = -1.0$, Figure 5).[19] The negative sign of ρ and the good correlation with σ^+ values are indicative of an electron transfer from the sulfide to the oxo-metalloporphyrin intermediate in the rate-determining step. The k_{BSA} constants of the same substrates exhibit similar Hammett correlation.[20] This observation indicates that the protein environment in the catalytic assembly does not perturb the electronic character of the sulfoxidation mechanism. Interestingly, a similar mechanism was suggested for the P-450-catalyzed sulfoxidation reactions.[2c]

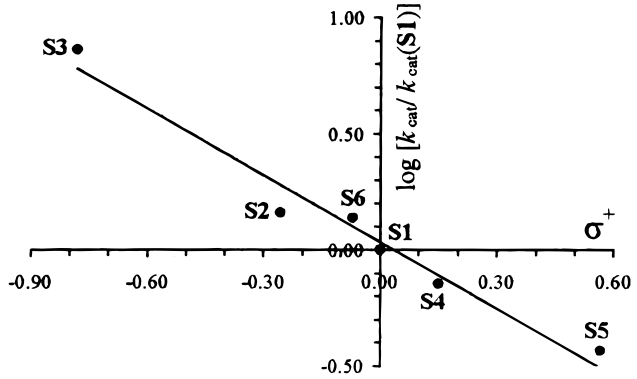

Figure 5. Hammett plot of the rate constants k_{cat} of sulfoxidation reactions catalyzed by the antibody−metalloporphyrin assembly.

Hammett plots of the two other reaction parameters, the Michaelis constant K_M and the enantiomeric excess, did not show any linear correlation with either σ or σ^+ values. Nevertheless, these parameters correlate between one another, with the more tightly bound substrate exhibiting higher enantioselectivity (Table 1). Apparently, both parameters are controlled primarily by steric rather than by electronic factors. The differences are probably dictated by the structure of the active site, which was predesigned to bind thioanisole **S1** rather than its substituted derivatives **S2**−**S7**. Thus, for example, **S2**, **S6**, and **S7**, which differ from **S1** (the best binder and also the best substrate in terms of ee) by just one methyl group, are characterized by diminished binding and reduced enantioselectivity. It is remarkable that such a catalytic assembly, induced by one of the largest haptens ever used to elicit catalytic antibodies, can sense very small structural variations in the substrate.

In summary, we have demonstrated for the first time that an antibody−metalloporphyrin catalytic assembly can be designed not only to catalyze oxygenation reactions but also to exhibit other enzyme characteristics, such as predetermined oxidant and substrate selectivity, enantioselective delivery of oxygen to the substrate, and Michaelis−Menten saturation kinetics. This cofactor-bearing antibody, which promotes a complex, multistep catalytic event, represents a close model of the natural heme-dependent oxidation enzymes. Further characterization of this catalytic assembly is currently underway.

Experimental Section

^{1}H NMR spectra were recorded on a Bruker AM200, operating at 200 MHz. X-ray crystallographic analysis was performed on a Philips PW 110/20 four-circle diffractometer. HPLC analyses were carried out with a Merck-Hitachi Lachrom system equipped with an L-7100 pump, an L-7400 UV−vis detector, and a D-7000 system manager. Thioanisole

(19) σ and σ^+ values were adopted from: (a) Gordon, A. J.; Ford, R. A. *The Chemist's Companion*; Wiley-Interscience: New York, 1972; pp 145−155. (b) *Advances in Linear Free Energy Relationships*; Chapman, N., Shorter, J., Eds.; Plenum Press: New York, 1972; pp 455−484.

(20) In contrast, the k_{uncat} constants correlate with σ rather than with σ^+ values ($\rho = -1.5$); i.e., in the absence of porphyrin, a concerted nucleophilic attack of the sulfide on PhIO takes place.

(**S1**), methyl *p*-tolyl sulfide (**S2**), 1-methoxy-4-(methylthio)benzene (**S3**), 4-bromothioanisole (**S4**), 4-(methylthio)acetophenone (**S5**), ethyl phenyl sulfide (**S7**), and benzyl phenyl sulfide (**S8**) were purchased from Aldrich. Methyl *m*-tolyl sulfide (**S6**) and 1-(methylthio)naphthalene (**S9**) were prepared from their corresponding thiols.[21] Iodosylbenzene was prepared from diacetoxy iodobenzene.[22] $NaIO_4$ was purchased from Aldrich.

[*meso*-Tetrakis(4-carboxyphenyl)porphinato]tin(IV) α-Naphthoxide Chloride (P1). Compound **P2** (100 mg, 0.1 mmol) was dissolved in pyridine (10 mL), excess α-naphthol (1 g, 6.9 mmol) was added, and the solution was refluxed for 5 h. The solvent was removed under reduced pressure, and the residue was triturated with acetone (40 mL), filtered, and washed with acetone to give a purple powder (80 mg) that was found (by ^{1}H NMR) to be a 1:1 mixture of **P1** and unreacted **P2**. Taking into account the versatility of the immune response and the option to screen for the desired antibodies, this mixture was not separated prior to conjugation with the carrier proteins and immunization. ^{1}H NMR of **P1** (D_2O): δ 9.09 (s, 8H, pyrrole), 8.25 (d, $J = 8$ Hz, 8H), 8.15 (d, $J = 8$ Hz, 8H), 6.92 (d, $J = 8$ Hz, 1H), 6.70 (t, $J = 8$ Hz, 1H), 6.20 (m, 2H), 5.73 (t, $J = 8$ Hz, 1H), 2.35 (d, $J = 8$ Hz, 1H), 1.14 (d, $J = 8$ Hz, 1H).

[*meso*-Tetrakis(4-carboxyphenyl)porphinato]tin(IV) Dichloride (P2). Stannation of the free base porphyrin, tcpp-H_2,[23] was carried out as described earlier.[13] ^{1}H NMR (D_2O): δ 9.16 (s, 8H, pyrrole), 8.25 (d, $J = 8$ Hz, 8H), 8.15 (d, $J = 8$ Hz, 8H).

[*meso*-Tetrakis(4-tolyl)porphinato]tin(IV) Di(α-naphthoxide) (P3). Using the above-described synthesis of **P1**, compound **P3** was prepared from [*meso*-tetrakis(4-tolyl)porphinato]tin(IV) dichloride.[13,24] Compound **P3** was recrystallized from CH_2Cl_2−hexane. ^{1}H NMR ($CDCl_3$): δ 9.00 (s, 8H), 7.82 (d, $J = 8$ Hz, 8H), 7.55 (d, $J = 8$ Hz, 8H), 6.92 (d, $J = 8$ Hz, 2H), 6.70 (t, $J = 8$ Hz, 2H), 6.15 (m, 4H), 5.75 (t, $J = 8$ Hz, 2H), 2.79 (d, $J = 8$ Hz, 2H), 2.71 (s, 12H), 1.33 (d, $J = 8$ Hz, 2H). Crystallographic data: empirical formula $C_{68}H_{50}N_4O_2Sn$, fw 1073.81; crystal system trigonal, space group *R*-3, purple plates; $a = 37.73(2)$ Å, $c = 10.323(5)$ Å; $T = 293$ K; $z = 9$; final *R* indices [$I > 2\sigma(I)$], $R1 = 0.0948$, $wR2 = 0.1715$; GOF = 0.967; $\lambda = 0.7107$ Å; 2θ range for data collection 4−48°; number of reflections used for refinement, 4059 [$I > 2\sigma(I)$]; number of parameters refined, 334; calculated density, 1.261 g/cm^3; intensity measurement method, $\omega/2\theta$.

[*meso*-Tetrakis(4-bromophenyl)porphinato]tin(IV) Di(α-naphthoxide) (P4). Using the above-described synthesis of **P1**, compound **P4** was prepared from [*meso*-tetrakis(4-bromophenyl)porphinato]tin(IV) dichloride.[13,24] Compound **P4** was recrystallized from CH_2Cl_2−hexane. ^{1}H NMR ($CDCl_3$): δ 9.00 (s, 8H), 7.92 (d, $J = 8$ Hz, 8H), 7.82 (d, $J = 8$ Hz, 8H), 6.93 (d, $J = 8$ Hz, 2H), 6.72 (t, $J = 8$ Hz, 2H), 6.18 (m, 4H), 5.73 (t, $J = 8$ Hz, 2H), 2.70 (d, $J = 8$ Hz, 2H), 1.27 (d, $J = 8$ Hz, 2H).

[*meso*-Tetrakis(4-carboxyphenyl)porphinato]ruthenium(II) Carbonyl (P5). Insertion of ruthenium(II) carbonyl to *meso*-tetrakis(4-carbomethoxyphenyl)porphyrin[24] was carried out using a known procedure.[25] The resultant Ru(II) porphyrin (80 mg) was treated with a boiling mixture of 3 N KOH−methanol (1:1, 60 mL) for 2 h. Acidification followed by filtration of the resultant orange precipitate produced **P5** (70 mg) in the form of a dark powder. ^{1}H NMR (DMSO-d_6): δ 8.70 (s, 8H, pyrrole), 8.40 (m, 16H).[26]

Immunization and Antibody Production. Hapten **P1** was conjugated to the carrier proteins, KLH and BSA, by activation of its carboxylic groups with EDC and NHS.[14] Balb/C mice were immunized with the KLH conjugate in complete Freund's adjuvant. Mice with a serum titer of 1:6000 were used to generate hybridomas by fusion of their spleen cells with myeloma cells.[15] Three hybridoma cells producing anti-**P1** antibodies were selected on the basis of ELISA tests for further studies.[16] Antibodies from each cell line were produced in larger amounts from ascites fluid and then purified by ammonium sulfate precipitation and protein-G affinity chromatography. Antibody SN37.4, which exhibited the highest values of enantioselectivity in the sulfoxidation of **S1**, was selected for the kinetic studies.

Kinetics and Enantioselectivity Studies of Sulfoxidation Reactions. Metalloporphyrin **P5** (5×10^{-7} M) was added to an aqueous solution of the appropriate protein, either antibody SN37.4 (1 mg/mL, 6.7×10^{-6} M) or BSA (1 mg/mL, 1.5×10^{-5} M) in carbonate buffer (50 mM, 100 mM NaCl, pH 9.0), and the mixture was left at 4 °C for 2 h. In experiments where an inert porphyrin was also used, it was added at this stage as well (**P2**, 5×10^{-5} M). An acetonitrile solution of organic substrate was added in the appropriate amount to reach 4% acetonitrile and substrate concentration between 5×10^{-4} and 5×10^{-2} M. Similarly, methanolic solution of PhIO was added to reach a concentration of 5×10^{-4} M and 2% methanol. Acetonitrile solution of 1,3-dinitrobenzene (internal standard) was added to reach a concentration of 5×10^{-6} M with additional 2% acetonitrile (total organic cosolvent 8%). The reaction was kept at 4 °C and monitored by HPLC equipped with an RP-18 column (Merck Lichrospher). Initial rates were measured at 5−10% conversion with respect to PhIO. Typical yields in the presence of **P5** were 70−80% with respect to PhIO, i.e., 700−800 catalytic turnovers. The product's enantiomeric excess was determined for reactions with 5×10^{-4} M substrate. The product was extracted with CH_2Cl_2 prior to HPLC analysis using a chiral column (Merck Whelk-O1).

Acknowledgment. We thank the Israel Science Foundation, the US-Israel Binational Science Foundation, and the Skaggs Institute for Chemical Biology for financial support. We thank Tami Danon and Prof. Zelig Eshhar for antibody preparation, and Dr. Moshe Kapon for the X-ray crystallographic studies. E.K. is the incumbent of the Benno Gitter & Ilana Ben-Ami chair of Biotechnology, Technion.

Supporting Information Available: ^{1}H NMR spectra of hapten **P1** after 48 h under physiological conditions (50 mM phosphate buffer, pH 7.4, 100 mM NaCl, 37 °C) and of compound **P4** (PDF). X-ray structural information and an X-ray crystallographic file (CIF) of compound **P3** are also available. This material is available free of charge via the Internet at http://pubs.acs.org.

JA990314Q

(21) Ono, N.; Miyake, H.; Saito, T.; Kaji, A. *Synthesis* **1980**, 952.
(22) Saltzman, H.; Sharefkin, G. *Organic Syntheses*; Wiley: New York, 1955; Collect. Vol. III, p 658.
(23) Longo, F. R.; Finarelly, M. G.; Kim, J. B. *J. Heterocycl. Chem.* **1969**, *6*, 927.
(24) Datta-Gupta, N.; Bardos, T. J. *J. Heterocycl. Chem.* **1966**, *3*, 495.
(25) Le Maux, P.; Bahri, H.; Simonneaux, G. *Tetrahedron* **1993**, *49*, 1401.
(26) In agreement with: Hartmann, M.; Robert, A.; Durate, V.; Keppler, B. K.; Meunier, B. *J. Biol. Inorg. Chem.* **1997**, *2*, 427.